Effect of Direction of External Magnetic Field on Minimum Propagation Current of a Composite Conductor for LHD Helical Coils

Effect of Direction of External Magnetic Field on Minimum Propagation Current of A Composite Conductor for LHD Helical Coils

S. Imagawa, *IEEE Member*, H. Chikaraishi, *IEEE Member*, S. Hamaguchi, T. Obana, A. Iwamoto, N. Yanagi, K. Takahata, and T. Mito

***Abstract*—The conductor for helical coils of the Large Helical Device consists of a Rutherford-type NbTi/Cu cable, a pure aluminum stabilizer, and a copper sheath. The dimensions of the conductor and the stabilizer cross-sections are 18.0 mm × 12.5 mm and 12.4 mm × 5.2 mm, respectively. The measured cold-end recovery current in the magnetic field parallel to the shorter side (*B*//12.5) is clearly lower than that in the field parallel to the longer side (*B*//18.0) because of the difference in magnetoresistance by Hall currents. Since the minimum propagation current I_{mp} is important to determine the upper limit of operation current, I_{mp} has been measured for two types of one-turn coil samples, which were bent flatwise (*B*//18.0) and edgewise (*B*//12.5) with the inner radius of 0.14 m to extend the length in the uniform background field of the test facility. The measured I_{mp} at *B*//12.5 is almost the same as that at *B*//18.0 in spite of the large difference in the steady-state resistance. I_{mp} is considered to be determined by the heat balance before the current diffuses deeply into the stabilizer.**

***Index Terms*—aluminum stabilizer, cold-end recovery current, Hall current, magnetoresistance, minimum propagation current**

I. Introduction

HELICAL coils of the Large Helical Device (LHD) adopt a composite conductor that consists of a Rutherford-type NbTi/Cu cable, a pure aluminum stabilizer, and a copper sheath [1]. The conductors were supplied by Hitachi, Ltd. The copper sheath consists of a U-shaped part and a top cover, and they were welded after insertion of the cable and the stabilizer. The stabilizer is clad with a Cu-2%Ni layer of 0.4 mm thick for reduction of magnetoresistance induced by Hall currents flowing in the aluminum stabilizer through the copper sheath and the cable [2]-[5]. The dimensions of the conductor and the stabilizer cross-sections are 18.0 mm × 12.5 mm and 12.4 mm × 5.2 mm, respectively. Since the Hall voltage is proportional to the length of the material across the magnetic field, the magnetoresistance of the conductor is the highest in the magnetic field parallel to the shorter side (*B*//12.5).

The LHD helical coil was designed to be cryostable, that is, the cold-end recovery current I_r is higher than the operation current of 13.0 kA. However, propagation of a normal zone has been observed several times in the first and second layers of the helical coils at higher than 11 kA that is obviously lower than I_r measured with conductor tests [6], [7]. Additional heat generation caused by slow current diffusion into the pure aluminum stabilizer is able to induce propagation of a normal zone at the current lower than I_r. The minimum propagation current I_{mp} is important for pool-cooled magnets to determine the upper limit of the operation current. Since the direction of the magnetic field in each conductor of the helical coil varies, the effect of the field direction on I_{mp} has been measured using two types of one-turn coil samples that were bent flatwise and edgewise. This paper intends to summarize the experimental results and to discuss the effect of Hall currents on I_{mp}.

II. Experimental Setup and Method

A. Samples and Setup

Coil-shaped samples were adopted to elongate the uniform field length. Two conductor samples were prepared. Sample-A was bent flatwise, and Sample-B was bent edgewise with the inner radius of 0.14 m, as shown in Fig. 1. The conductors were clamped with GFRP (Glass Fiber Reinforced Plastic) blocks with width of 22 mm by 51-52 mm pitch. Then, the wetted surface fraction was 57-58%, which was equivalent to those of the 2nd-4th layers of the LHD helical coils. The GFRP blocks were fixed from an inside ring support. Nichrome heaters and thermo-sensors were attached on the conductor with epoxy resin under the GFRP blocks. Longitudinal voltage taps VLA1-5 and VLB1-5 were attached on the conductor with solder to detect the transition to normal state. Since the positive pole of VLA3 was disconnected, the voltage between the negative pole of VLA3 and the negative pole of VLA4 was utilized as new VLA3. In addition, VLA5 was not available because of disconnection of the leading cable.

Sample-A and Sample-B were jointed in series, and they were installed into a test facility with a 9 T split coil [8], as shown in Fig. 2. The direction of background magnetic field

Manuscript received November 25, 2020. This work was supported by the NIFS Collaboration Research program (code NIFS10ULAA702).

S. Imagawa is with the National Institute for Fusion Science, Toki, Gifu 509-5292, Japan, phone: +81-572-58-2132, e-mail: imagawa@nifs.ac.jp.

H. Chikaraishi, S. Hamaguchi, T. Obana, A. Iwamoto, N. Yanagi, K. Takahata, and T. Mito are with the National Institute for Fusion Science, e-mail: hchikara@nifs.ac.jp, hamaguchi.shinji@nifs.ac.jp, obana.tetsuhiro@nifs.ac.jp, iwamoto@nifs.ac.jp, yanagi@nifs.ac.jp, takahata@nifs.ac.jp, mito@nifs.ac.jp.

Color versions of one or more of the figures in this paper are available online at http://ieeexplore.ieee.org.

Digital Object Identifier will be inserted here upon acceptance.

was parallel to the longer side (B//18.0) for Sample-A and to the shorter side (B//12.5) for Sample-B. The field strength at the conductors was 85% of the central field of the split coil. The samples were cooled with liquid helium.

B. Experimental Method

At first, the background field coil was charged. Secondly, the sample current was ramped up to the testing value. After that, the heater at the bottom position of the testing sample was excited from low power. The duration of the heat input was set at 0.02 s. The maximum heater power was 100 W. Propagation of a normal zone was detected with longitudinal voltage taps and thermo-sensors. The sampling rate was 1 kHz with low pass filter of 5 kHz. In the case that the normal zone stagnated, I_r was measured with decreasing the current by the rate of 20 A/s.

III. Experimental Results

A. Output of voltage taps and thermo-sensors

Example outputs of the voltage taps and the thermo-sensors of Sample-A and Sample-B are shown in Figs. 3 and 4, respectively. The outputs of voltage taps were affected by the shift of the transport current during transition between superconducting state and normal state. Since the route of the cable of VLA1 was outside of the coil-shaped sample, the inductive voltage caused by the inward shift of the transport current during propagation of a normal zone was positive, and its output was enlarged. On the contrary, the routes of the cables of VLA2-4 were inside, and their outputs were reduced by the inductive voltage. The routes of cables of VLB1-5 were outside. Since each surrounding area by the cable and the conductor was perpendicular to the direction of the current shift, the effect of the current shift on the voltage output was small.

In the case of Sample-A (B//18.0), normal zones propagated to only the downstream side of the current with recovery from the upstream side at currents slightly higher than a threshold current. They propagated to both sides at further high currents and also recovered to superconducting after the propagation stopped at the low field region at the terminals. Less than 13 kA at 6.81 T, 14 kA at 5.96 T, or 15 kA at 5.11 T, all normal zones were recovered, that is, these currents were lower than I_r. Propagation velocity in the downstream side of the current was faster than that in the opposite side. Necessary heating power for propagation of a normal zone is shown in Fig. 5. Propagation occurred at the current higher than the threshold value that is lowered with increasing the field. In some range of currents, one-side or both-side propagation depends on heater power, as shown in Figs. 3a and 3b. The initial length of the normal zone should depend on the heater power.

In the case of Sample-B (B//12.5), most of the normal zones propagated to both sides and stagnated, as shown in Fig. 4b. I_r was measured with decreasing the current after stagnation of the normal zones. One-side propagation or stagnation of a short normal zone occurred around the threshold current, as shown in Fig. 4a. Propagation velocity in the downstream side

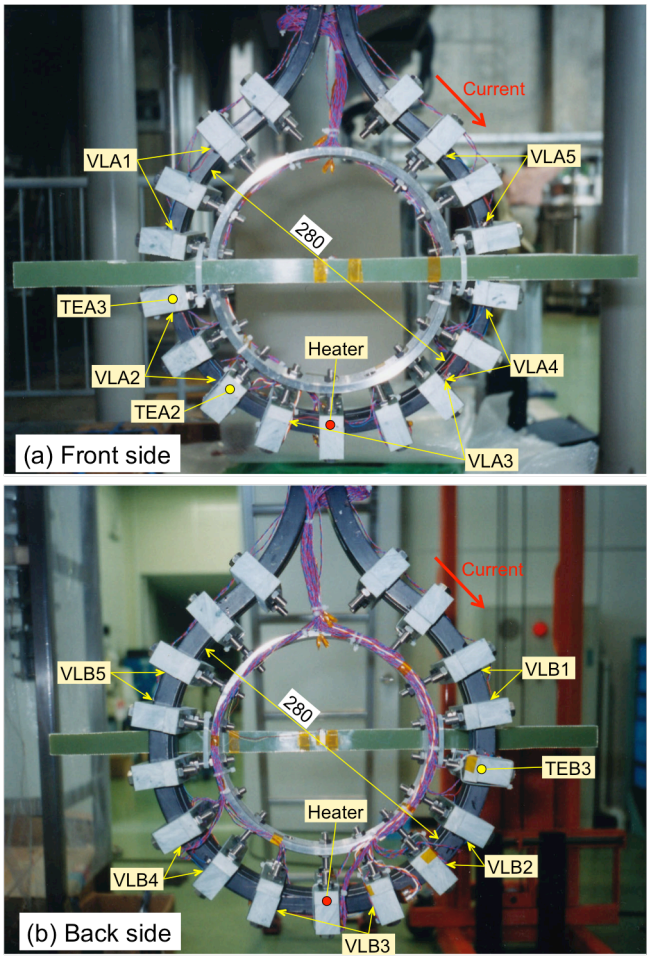

Fig. 1. (a) A photo of Sample-A. (b) A photo of Sample-B.

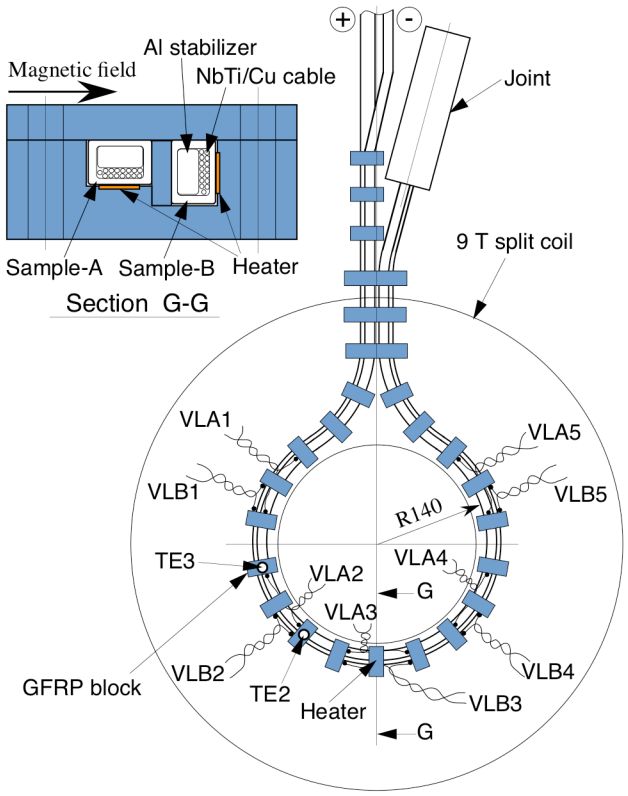

Fig. 2. A sketch of the assembly of Sample-A and Sample-B.

of the current was almost the same as that in the upstream side. The threshold current of Sample-B for propagation of a normal zone at each field was almost the same as that of Sample-A, as shown in Fig. 5.

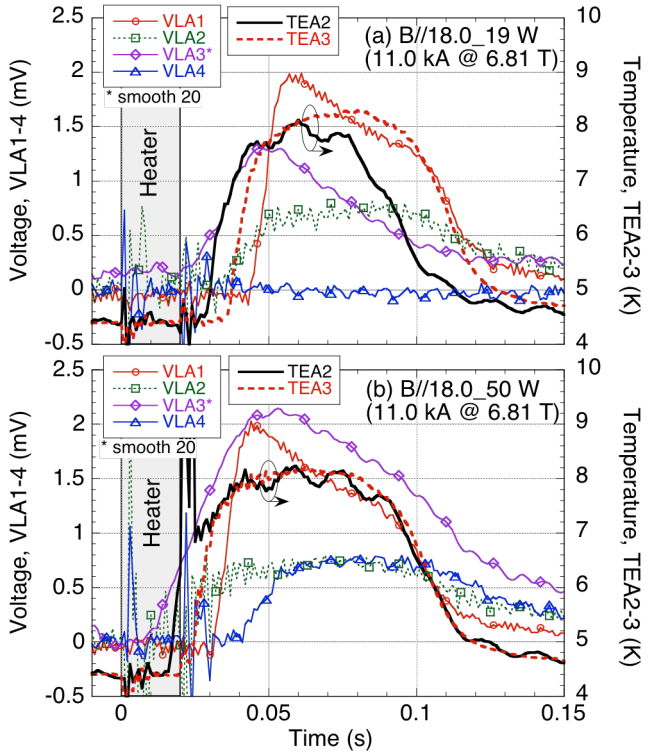

Fig. 3. Voltages and temperatures during propagation of a normal zone in Sample-A in the case of (a) 11.0 kA at 6.81 T with 19 W and (b) 11.0 kA at 6.81 T with 50 W. Smoothing by 20 points was adopted for only VLA3.

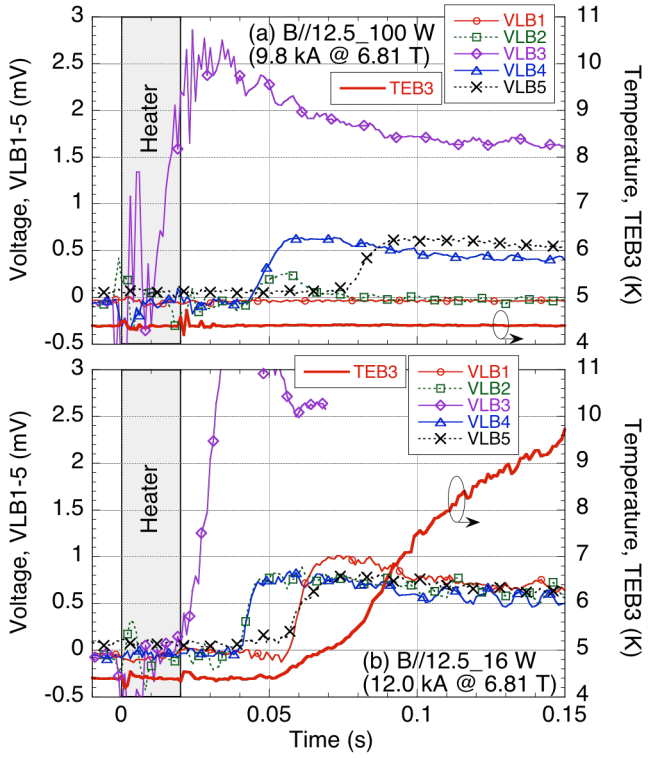

Fig. 4. Voltages and temperatures during propagation of a normal zone in Sample-B in the case of (a) 9.8 kA at 6.81 T with 100 W and (b) 12.0 kA at 6.81 T with 16 W. Smoothing by 5 points was adopted for VLB1-5.

B. *Minimum propagation current*

The minimum heat input for propagation increased as the current decreased in the same background field, as shown in Fig. 5, and it increased sharply at a certain current, which can be defined as I_{mp}. The heater power of 100 W (2 J) should be sufficient heat input at higher field than 5.11 T. I_r and I_{mp} of Sample-A and Sample-B are shown in Fig. 6. In this setup, I_{mp} of Sample-B is higher than I_r. The length of normal zones induced with the heater is considered to be limited within two pitches even in the case of 100 W, because the thermo-sensor TEA2 changed only when a normal zone propagated. According to Fig. 6, I_{mp} of Sample-A and I_{mp} of Sample-B are almost the same in spite of the great difference in I_r. Therefore, I_{mp} is considered to be determined by the heat balance before the magnetoresistance by Hall currents becomes dominant.

C. *Propagation velocity*

Propagation velocities of Sample-A and Sample-B are shown in Figs. 7 and 8, respectively. Downstream velocity of Sample-A was almost twice the upstream velocity, which is consistent with the references [9]-[13]. This asymmetrical velocity is considered to be caused by electric field induced by the transfer current across the external field [14]. Downstream propagation velocity of Sample-B was almost the same as the upstream velocity, and this value was comparable to the average velocity of downstream and upstream of Sample-A at the

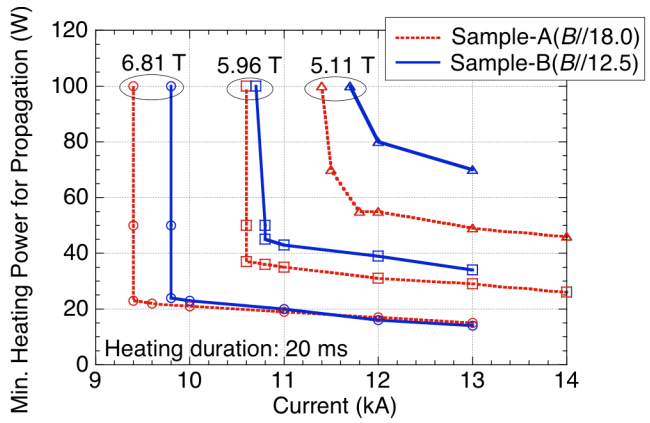

Fig. 5. Minimum heating power for propagation of a normal zone in Sample-A and Sample-B.

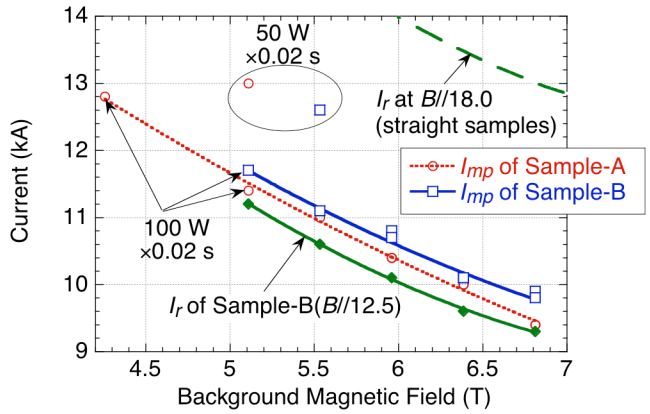

Fig. 6. Minimun propagation current I_{mp} and cold-end recovery current I_r. I_r at B//18.0 was measured with straight samples [1].

same current and field. Minimum velocity of Sample-A was 5 m/s, and Sample-B was 3.5 m/s. It took less than 0.015 s for a normal zone to propagate to the next uncooled area under the GFRP block.

D. *Steady-state Resistance*

Steady-state resistances after current diffusion are shown in Fig. 9 in comparison with the calculation [4]. The resistance of Sample-B was three times as high as that of Sample-A. The main cause was the difference in height of the aluminum stabilizer. Field dependence of the resistance was in good accordance with the calculation. According to the calculation, contact resistance in the Hall current circuit in Sample-A was quite high. The contact resistance between CuNi layer and NbTi/Cu cable or Cu cover should be high in Sample-A.

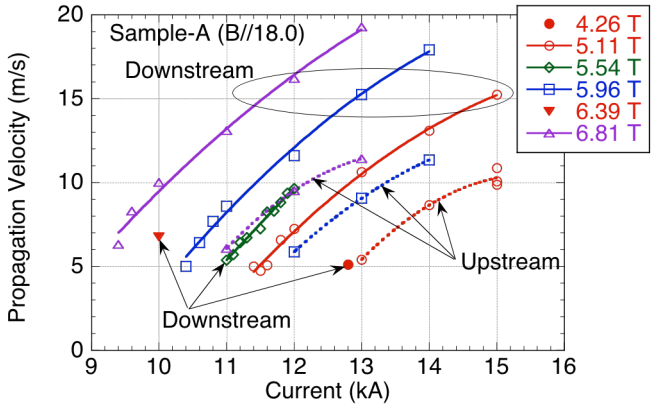

Fig. 7. Propagation velocity of Sample-A. Dashed lines show upstream velocities, and the others show downstream velocities.

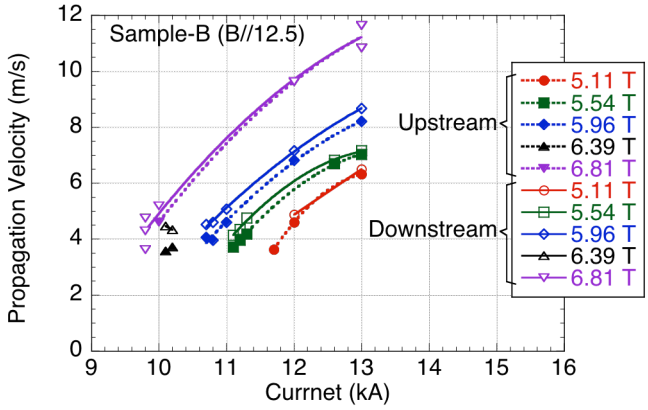

Fig. 8. Propagation velocity of Sample-B.

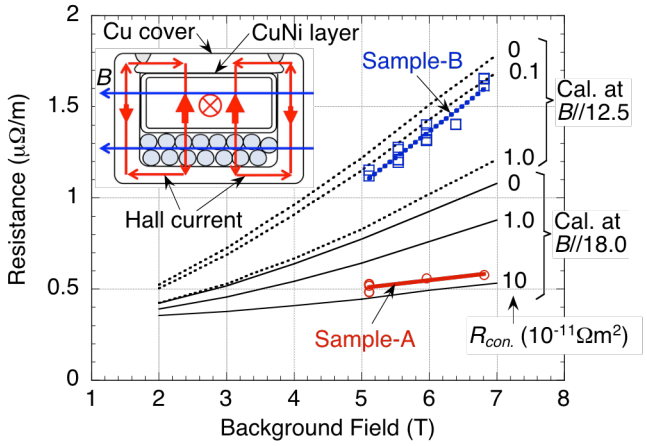

Fig. 9. Resistance per unit length after current diffusion into aluminum stabilizer. $R_{con.}$ is sum of contact resistance in the Hall current circut [4].

IV. Discussion

Heat generation during current diffusion into aluminum can be calculated analytically [15], [16], and the time dependence of resistance is expressed by exponential function. For example, the resistance at 6.13 T (*B*//18.0) of the Model Coil of the LHD helical coil [17] is fitted by

$$\rho = 0.67 + 1.07\exp(-t/0.059) \quad (1)$$

where ρ (μΩ/m) and t (s) are resistance per unit length and time [7], which means that the steady-state resistance is 0.67 μΩ/m. In the case of Sample-B, the steady-state resistance at 6.13 T is 1.4 μΩ/m from Fig. 9. ρ in (1) becomes this value at t of 0.022 s which is longer than the time for a normal zone to propagate to the next uncooled area. Since the heat generation due to current diffusion is considered to be independent of the direction of magnetic field, the heat generation at the beginning of current diffusion should be the same between Sample-A and Sample-B. I_{mp} should be determined by the heat balance before the magnetoresistance becomes dominant.

I_{mp} of Sample-A and Sample-B are in good accordance with those of the conductors in the first and second layers of the LHD helical coils as well as the Model Coil in spite of the large deviation of the magnetoresistance that varies with the contact resistances in the conductors. Therefore, we can conclude that the effect of the direction of the magnetic field on I_{mp} can be neglected for the LHD helical coils.

V. Summary

The minimum propagation currents of a composite conductor of the LHD helical coil have been measured with coil-shaped conductor samples under the background field up to 6.81 T. Sample-A was bent flatwise (*B*//18.0), and Sample-B was bent edgewise (*B*//12.5). The steady-state resistance of Sample-B is three times higher than Sample-A because of the difference in magnetoresistance due to rectangular shape of the aluminum stabilizer. In spite of the large difference in magnetoresistance, their measured minimum propagation currents are almost the same. The minimum propagation current is considered to be determined by the heat balance before the magnetoresistance becomes dominant than the additional heat generation due to the current diffusion.

References

[1] N. Yanagi, T. Mito, S. Imagawa, K. Takahata, T. Satow, J. Yamamoto, O. Motojima, and The LHD Group, "Development and quality control of the superconductors for the helical coils of LHD," *Fusion Eng. Des.*, vol. 41, 1998, pp. 241-246.

[2] N. Yanagi, A.V. Gavrilin, T. Mito, S. Imagawa, K. Takahata, A. Iwamoto, H. Chikaraishi, S. Yamaguchi, T. Satow, S. Satoh, and O.

Motojima, "Stability characteristics of the aluminum stabilized superconductor for the LHD helical coils," *Advances in Superconductivity* XI, 1999, pp. 991-994.

[3] N. Yanagi, S. Imagawa, A.V. Gavrilin, T. Mito, A. Iwamoto, H. Chikaraishi, S. Hamaguchi, A. Nishimura, T. Satow, Y. Nakamura, S. Satoh, and O. Motojima, "Analysis of the normal transition event of the LHD helical coils," *IEEE Trans. Appl. Supercond.*, vol.10, no.1, 2000, pp. 610-613.

[4] S. Imagawa, N. Yanagi, T. Mito, T. Satow, J. Yamamoto, O. Motojima, and LHD group, "Analysis of anomalous resistivity in an aluminium stabilized superconductor for the Large Helical Device," *Advances in Cryogenic Eng.*, vol. 40A, 1994, pp. 469-477.

[5] V.S. Vysotsky, Yu.A. Ilyin, S. Sato, M. Takeo, N. Yanagi, A.V. Gavrilin, S. Imagawa, A. Iwamoto, S. Hamaguchi, T. Mito, T. Satow, S.Satoh, O. Motojima, "Temperature and electric field distribution measurement inside of the LHD helical conductor", *IEEE Trans. Appl. Supercond.*, vol. 10, no. 1 (2000) pp. 1259-1262.

[6] S. Imagawa, N. Yanagi, H. Chikaraishi, T. Mito, K. Takahata, S. Hamaguchi, H. Sekiguchi, S. Yamada, T. Satow, Y. Nakamura, S. Satoh, and O. Motojima, "Results of the first excitation of helical coils of the Large Helical Device," *IEEE Trans. Appl. Supercond.*, vol. 10, April 2000, pp. 606-609.

[7] S. Imagawa, N. Yanagi, and T. Mito, "Reconsideration of evaluation of balance voltages during a normal zone propagation in the LHD helical coils," *IEEE Trans. Appl. Supercond.*, vol. 23, June 2013, Art. no. 4700904.

[8] J. Yamamoto, T. Mito, K. Takahata, S. Yamada, N. Yanagi, I. Ohtake, A. Nishimura, and O. Motojima, "Superconducting test facility of NIFS for the Large Helical Device," *Fusion Eng. Des.*, vol. 20, January 1993, pp. 147–151.

[9] N. Yanagi, T. Mito, K. Takahata, M. Sakamoto, A. Nishimura, S. Yamada, S. Imagawa, H. Kaneko, J. Yamamoto, and O. Motojima, "Experimental observation of anomalous magnetoresistivity in 10 - 20 kA class aluminum stabilized superconductors," *Advances in Cryogenic Eng*., vol. 40, 1994, pp. 459-468.

[10] N. Yanagi, S. Imagawa, Y. Hishinuma, K. Seo, K. Takahata, S. Hamaguchi, A. Iwamoto, H. Chikaraishi, H. Tamura, S. Moriuchi, S. Yamada, A. Nishimura, T. Mito, and O. Motojima; "Asymmetrical normal-zone propagation observed in the aluminum-stabilized superconductor for the LHD helical coils," *IEEE Trans. Appl. Supercond.,* vol. 14, no. 2, June 2004, pp. 1507-1510.

[11] M. Ohya, Y. Shirai, M. Shiotsu, and S. Imagawa, "Effect of surface oxidation on stability of LHD conductor immersed in pressurized HeII", *IEEE Trans. Appl. Supercond.*, vol. 16, no. 2, June 2006, pp. 739-742.

[12] R. Ikuta, M. Ohya, Y. Shirai, M. Shiotsu, and S. Imagawa, "Transient stability of large helical device conductor with and without aluminum stabilizer (1) - experimental results", *IEEE Trans. Appl. Supercond.*, vol. 17, no. 2, June 2007, pp. 2454-2457

[13] Y. Shirai, R. Ikuta, T. Goto, M. Ohya, M. Shiotsu, S. Imagawa; "Transient stability analysis of large scale aluminum stabilized superconductor cooled by He II", *IEEE Trans. Appl. Supercond.*, vol. 18, no. 2, June 2008, pp. 1275 - 1279.

[14] S. Imagawa, "Dynamic analysis of the propagation velocity of the LHD helical coil," *Proceedings of the 24th International Cryogenic Engineering Conference and International Cryogenic Material Conference 2012*, Fukuoka, Japan, May. 14-18, 2012 (2013) pp. 591-594.

[15] A. Devred, "Investigation of current redistribution in superstablized superconducting winding when switching to the normal resistive state," *J. Appl. Phys*., vol. 65, 1989, pp. 3963-3967.

[16] A. Lee, R. H. Wands, and R. W. Fast, "Study of current redistribution in aluminum stabilized superconductor," *Cryogenics*, vol. 32, 1992, pp. 863-866.

[17] S. Imagawa, N. Yanagi, Y. Hishinuma, T. Mito, K. Takahata, H. Chikaraishi, H. Tamura, A. Iwamoto, S. Hamaguchi, K. Seo, S. Yamada, A. Nishimura, and O. Motojima, "Results of stability test in subcooled helium for the R&D coil of the LHD helical coil," *IEEE Trans. Appl. Supercond.,* vol. 14, no. 2, June 2004, pp. 1511-1514.